Phys. Lett. B 851 (2024) 138562

Contents lists available at ScienceDirect

Physics Letters B

journal homepage: www.elsevier.com/locate/physletb

Letter

Heavy axial-vector structures $bb\overline{c}\overline{c}$

S.S. Agaev [a], K. Azizi [b,c,*], H. Sundu [d]

[a] Institute for Physical Problems, Baku State University, Az–1148 Baku, Azerbaijan
[b] Department of Physics, University of Tehran, North Karegar Avenue, Tehran 14395-547, Iran
[c] Department of Physics, Doğuş University, Dudullu-Ümraniye, 34775 Istanbul, Türkiye
[d] Department of Physics Engineering, Istanbul Medeniyet University, 34700 Istanbul, Türkiye

ARTICLE INFO

Editor: A. Ringwald

ABSTRACT

The fully heavy axial-vector diquark-antidiquark structures $bb\overline{c}\overline{c}$ are explored by means of the QCD sum rule method. They are modeled as four-quark mesons T_1 and T_2 composed of $b^T C\sigma_{\mu\nu}\gamma_5 b$, $\overline{c}\gamma^\nu C\overline{c}^T$ and $b^T C\gamma_\mu\gamma_5 b$, $\overline{c}C\overline{c}^T$ diquarks, respectively. The spectroscopic parameters of the tetraquarks T_1 and T_2 are determined in the context of the QCD two-point sum rule method. Results obtained for masses of these states $m_1 = (12715 \pm 86)$ MeV and $m_2 = (13383 \pm 92)$ MeV are used to fix their strong decay channels. The full width $\Gamma(T_1)$ of the diquark-antidiquark state T_1 is estimated by considering the processes $T_1 \to B_c^- B_c^{*-}$ and $T_1 \to B_c^{*-} B_c^{*-}$. The decays to mesons $B_c^- B_c^{*-}$, $B_c^-(2S) B_c^{*-}$ and $B_c^{*-} B_c^{*-}$ are employed to evaluate $\Gamma(T_2)$. Results obtained for the widths $\Gamma(T_1) = (44.3 \pm 8.8)$ MeV and $\Gamma(T_2) = (82.5 \pm 13.7)$ MeV of these tetraquarks in conjunction with their masses are useful for future experimental studies of fully heavy resonances.

1. Introduction

The exotic four-quark mesons containing only heavy b or c quarks and their properties were already under consideration of researchers. This interest intensified after discoveries of four X resonances by the LHCb, ATLAS, and CMS Collaborations [1–3]. These new structures were observed in $J/\psi J/\psi$ and $J/\psi\psi'$ mass distributions and occupy $6.2 - 7.3$ GeV mass positions in the hadron spectroscopy. They are presumably fully charmed tetraquarks investigated in Refs. [4–20] though there are alternative explanations in literature as well [21,22].

Another class of fully heavy structures are exotic mesons $bb\overline{c}\overline{c}/cc\overline{b}\overline{b}$. They are interesting objects because some of them with masses below the relevant B_cB_c thresholds may be stable against strong decays. It is clear that such tetraquarks transform to conventional particles only through electroweak processes, and should have considerably longer lifetime. In this aspect $bb\overline{c}\overline{c}/cc\overline{b}\overline{b}$ differ from the tetraquarks $bb\overline{b}\overline{b}$ and $cc\overline{c}\overline{c}$: due to $b\overline{b}$ and $c\overline{c}$ annihilations they are strong-interaction unstable even residing below two-particle bottomonia (or charmonia) production limits [7,8,19].

The next reason to explore the tetraquarks $bb\overline{c}\overline{c}/cc\overline{b}\overline{b}$ is two units of electric charge that these particles bear. The existence of double-charged tetraquarks was predicted in Refs. [23,24], in which the authors calculated masses and partial widths of some of their decay modes. Such structures were analyzed in a detailed form in Refs. [25,26] as well. The first double-charged tetraquark seen in experiment is the scalar resonance $T^a_{cs0}(2900)^{++}$ observed recently by the LHCb Collaboration [27,28]. It has the quark content $cu\overline{s}\overline{d}$ and is also a fully open-flavor four-quark system. It is worth noting that the fully open-flavor tetraquarks were originally studied in the diquark-antidiquark model in Refs. [29,30].

The heavy tetraquarks $bb\overline{c}\overline{c}$ were already considered in the framework of various methods [31–37], in which the authors investigated different aspects of their physics. In fact, the masses of particles with $J^{\mathrm{P}} = 0^+$, 1^+ and 2^+ were evaluated in the color-magnetic interaction model in Ref. [31] and found above the B_cB_c threshold 12549 MeV. Weak decays of the scalar tetraquark $bb\overline{c}\overline{c}$ were analyzed in Ref. [32]. The mass spectra of fully heavy tetraquark states were calculated in two nonrelativistic quark models which contain one gluon exchange, linear confinement and hyperfine potentials [33]. In accordance to these studies the structures $bb\overline{c}\overline{c}$ with the quantum numbers $J^{\mathrm{P}} = 0^{++}$, 1^{+-} and 2^{++} reside above the B_cB_c thresholds. The masses of the scalar, axial-vector and tensor tetraquarks $bb\overline{c}\overline{c}$ within a potential model were found equal to 12947 MeV, 12960 MeV and 12972 MeV, respectively, which demonstrate their strong-interaction unstable nature [34]. In the relativistic quark model, this problem was addressed recently in Ref. [35], in which masses of the $J^{\mathrm{P}} = 0^+$, 1^+ and 2^+ diquark-antidiquark states

* Corresponding author.
E-mail address: kazem.azizi@ut.ac.ir (K. Azizi).

https://doi.org/10.1016/j.physletb.2024.138562
Received 10 January 2024; Received in revised form 13 February 2024; Accepted 4 March 2024

Available online 8 March 2024

$bb\overline{cc}$ were evaluated as 12848 MeV, 12852 MeV and 12859 MeV, respectively: All of these particles are above the relevant B_cB_c thresholds.

But analyses carried out using QCD moment sum rule method led to conclusions that certain structures $cc\overline{bb}$ with $J^{\rm P}=0^+$, 1^+ and 2^+ are strong-interaction stable states [36]. As a result, such tetraquarks can transform to ordinary particles only through electroweak processes. The same structures were investigated in the context of the dynamical diquark model and predicted to be stable against strong decays as well [37].

In our article [38], we explored the scalar tetraquarks X_1, $X_2=bb\overline{cc}$ composed of axial-vector and pseudoscalar diquarks, respectively. The masses of these states (12715 ± 80) MeV and (13370 ± 95) MeV overshoot the threshold for production of $B_c^-B_c^-$ mesons. This means that the scalar tetraquarks X_1 and X_2 with different internal organizations are strong-interaction unstable particles. We evaluated also their full widths by considering the strong decay channels $X_1\to B_c^-B_c^-$ and $B_c^{*-}B_c^{*-}$, and $X_2\to B_c^-B_c^-$, $B_c^-B_c^-(2S)$, and $B_c^{*-}B_c^{*-}$, respectively. Our predictions for the full widths of these states $\Gamma_1=(63\pm 12)$ MeV and $\Gamma_2=(79\pm 14)$ MeV allowed us to interpret them as tetraquarks with moderate width.

In the present article, we continue our investigations of the fully heavy tetraquarks by analyzing the axial-vector particles $bb\overline{cc}$. We model the tetraquark T_1 as an exotic meson with structure $C\sigma_{\mu\nu}\gamma_5\otimes\gamma^\nu C$ built of a diquark $b^TC\sigma_{\mu\nu}\gamma_5 b$ and antidiquark $\overline{c}\gamma^\nu C\overline{c}^T$. The tetraquark T_2 has the composition $C\gamma_\mu\gamma_5\otimes C$ and contains a vector diquark and pseudoscalar antidiquark. The states T_1 and T_2 have color triplet $\overline{\mathbf{3}}_c\otimes\mathbf{3}_c$ and sextet $\mathbf{6}_c\otimes\overline{\mathbf{6}}_c$ structures, respectively. The spectroscopic parameters of these tetraquarks are computed in the framework of the QCD sum rule (SR) approach [39,40]. To find widths of T_1 and T_2, we invoke the three-point SR method which is required to evaluate the strong couplings of $T_{1(2)}$ and final state-mesons B_cB_c with appropriate spin-parities and charges.

This work is composed in the following manner: In Sec. 2, we compute the spectroscopic parameters of the axial-vector tetraquarks T_1 and T_2. Using obtained predictions for masses of these systems, we determine their kinematically allowed decay channels. In Sec. 3, we consider decay modes of T_1 and compute its full width. The section 4 is devoted to analysis of decays of the structure T_2. Our concluding notes are presented in Sec. 5.

2. Mass and current coupling of T_1 and T_2

In this section, we calculate the mass $m_{1(2)}$ and current coupling $\Lambda_{1(2)}$ (a pole residue) of the axial-vector tetraquark $T_{1(2)}=bb\overline{cc}$ in the QCD two-point SR framework.

The SRs for the quantities m_1, Λ_1 and m_2, Λ_2 can be derived from analysis of the following correlator

$$\Pi_{\mu\nu}(p)=i\int d^4xe^{ipx}\langle 0|\mathcal{T}\{J_\mu(x)J_\nu^\dagger(0)\}|0\rangle. \tag{1}$$

Here $J_\mu(x)$ is an interpolating current of the particle under consideration. The symbol $\mathcal{T}$ is adopted for the time-ordering of two currents. To model the tetraquarks T_1 and T_2, we use the currents

$$J_\mu^1(x)=[b_a^T(x)C\sigma_{\mu\nu}\gamma_5 b_b(x)][\overline{c}_a(x)\gamma^\nu C\overline{c}_b^T(x)], \tag{2}$$

and

$$J_\mu^2(x)=[b_a^T(x)C\gamma_\mu\gamma_5 b_b(x)][\overline{c}_a(x)C\overline{c}_b^T(x)]. \tag{3}$$

Let us consider in a detailed form computation of the parameters m_1 and Λ_1. The correlation function $\Pi_{\mu\nu}^1(p)$ can be presented using the physical parameters of the tetraquark T_1. Having inserted into Eq. (1) a full set of states with the spin-parities and contents of T_1, and carried out integration over x, we get

$$\Pi_{\mu\nu}^{1\rm Phys}(p)=\frac{\langle 0|J_\mu^1|T_1(p,\epsilon)\rangle\langle T_1(p,\epsilon)|J_\upsilon^{1\dagger}|0\rangle}{m_1^2-p^2}+\cdots. \tag{4}$$

In expression above, only the contribution of the ground-state particle is written down explicitly: Effects of higher resonances and continuum states are denoted by the dots.

For further detailing of $\Pi_{\mu\nu}^{1\rm Phys}(p)$, it is convenient to introduce the matrix element

$$\langle 0|J_\mu^1|T_1(p,\epsilon)\rangle=\Lambda_1\epsilon_\mu(p), \tag{5}$$

where ϵ_μ is the polarization vector of T_1. Then, it is easy to find $\Pi_{\mu\nu}^{1\rm Phys}(p)$ which is given by the formula

$$\Pi_{\mu\nu}^{1\rm Phys}(p)=\frac{\Lambda_1^2}{m_1^2-p^2}\left(-g_{\mu\nu}+\frac{p_\mu p_\nu}{m^2}\right)+\cdots. \tag{6}$$

In what follows, we are going to use the invariant amplitude $\Pi^{1\rm Phys}(p^2)$ corresponding to the structure $g_{\mu\nu}$.

The QCD side of the SRs for the parameters m_1 and Λ_1 is equal to

$$\begin{aligned}\Pi_{\mu\nu}^{1\rm OPE}(p)&=i\int d^4xe^{ipx}\left\{{\rm Tr}\left[\gamma^\theta\widetilde{S}_c^{b'b}(-x)\gamma^\delta S_c^{a'a}(-x)\right]\right.\\&\times\left[{\rm Tr}\left[S_b^{bb'}(x)\gamma_5\sigma_{\nu\delta}\widetilde{S}_b^{aa'}(x)\sigma_{\mu\theta}\gamma_5\right]\right.\\&-{\rm Tr}\left[S_b^{ab'}(x)\gamma_5\sigma_{\nu\delta}\widetilde{S}_b^{ba'}(x)\sigma_{\mu\theta}\gamma_5\right]\Big]+{\rm Tr}\left[\gamma^\theta\widetilde{S}_c^{a'b}(-x)\right.\\&\times\left.\gamma^\delta S_c^{b'a}(-x)\right]\left[{\rm Tr}\left[S_b^{ab'}(x)\gamma_5\sigma_{\nu\delta}\widetilde{S}_b^{ba'}(x)\sigma_{\mu\theta}\gamma_5\right]\right.\\&\left.\left.-{\rm Tr}\left[S_b^{bb'}(x)\gamma_5\sigma_{\nu\delta}\widetilde{S}_b^{aa'}(x)\sigma_{\mu\theta}\gamma_5\right]\right]\right\},\end{aligned} \tag{7}$$

where $\widetilde{S}_Q(x)=CS_Q^T(x)C$ with $S_{b(c)}(x)$ being the b and c-quark propagators [41]. We denote by $\Pi^{1\rm OPE}(p^2)$ the invariant amplitude which corresponds to the term $g_{\mu\nu}$ in the correlator $\Pi_{\mu\nu}^{1\rm OPE}(p)$.

The sum rules for the mass and current coupling of the tetraquark T_1 are given by the expressions

$$m_1^2=\frac{\Pi^{1\prime}(M^2,s_0)}{\Pi^1(M^2,s_0)} \tag{8}$$

and

$$\Lambda_1^2=e^{m_1^2/M^2}\Pi^1(M^2,s_0), \tag{9}$$

where $\Pi^1(M^2,s_0)$ is the amplitude $\Pi^{1\rm OPE}(p^2)$ after the Borel transformation and continuum subtraction procedures. Here M^2 and s_0 are the Borel and continuum subtraction parameters, respectively. In Eq. (8), we also adopt a notation $\Pi^{1\prime}(M^2,s_0)=d\Pi^1(M^2,s_0)/d(-1/M^2)$.

In numerical computations, we employ the input parameters

$$\begin{aligned}&\langle\alpha_sG^2/\pi\rangle=(0.012\pm 0.004)~{\rm GeV}^4,\\&\quad m_b=4.18^{+0.03}_{-0.02}~{\rm GeV},\\&\quad m_c=(1.27\pm 0.02)~{\rm GeV}.\end{aligned} \tag{10}$$

The auxiliary quantities M^2 and s_0 are chosen within limits

$$M^2\in[12,14]~{\rm GeV}^2,~~s_0\in[180,185]~{\rm GeV}^2, \tag{11}$$

which comply with all constraints of SR calculations. Indeed, at $M^2=14$ GeV^2 and $M^2=12$ GeV^2 on the average in s_0 the pole contribution is PC ≈ 0.5 and PC ≈ 0.64, respectively (see, Fig. 1). At $M^2=12$ GeV^2 the nonperturbative contribution is positive and forms 2% of the whole result.

The mass m_1 and current coupling Λ_1 are found as mean values of these parameters calculated at 10 different points from the regions Eq. (11). For example, the maximum $m_1=12800$ MeV is reached at $M^2=14$ GeV^2 and $s_0=185$ GeV^2, whereas m_1 gets its minimum value 12630 MeV at $M^2=12$ GeV^2 and $s_0=180$ GeV^2. As a result, we find

$$\begin{aligned}&m_1=(12714\pm 86)~{\rm MeV},\\&\Lambda_1=(2.27\pm 0.26)~{\rm GeV}^5.\end{aligned} \tag{12}$$

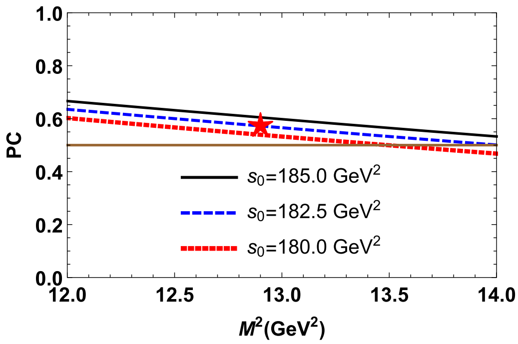

Fig. 1. The pole contribution PC as a function of the Borel parameter M^2 at different s_0. The horizontal line limits a region $\mathrm{PC}=0.5$. The red star marks the point, where the mass m of T_1 has effectively been computed.

Here, the errors are generated mainly by uncertainties in the choice of the parameters M^2 and s_0: Effects of ambiguities in Eq. (10) on the final output are small. The results in Eq. (12) effectively amount to the SR predictions at the point $M^2=12.9\ \mathrm{GeV}^2$ and $s_0=182.5\ \mathrm{GeV}^2$, where the pole contribution is $\mathrm{PC}\approx 0.57$. This fact guarantees the dominance of PC in the obtained results, and proves ground-level nature of T_1 in segment of axial-vector tetraquarks $bb\overline{c}\overline{c}$. The dependence of the mass m_1 on M^2 and s_0 is shown in Fig. 2.

The parameters of the tetraquark T_2 are determined by the similar manner. Below, we provide the correlation function $\Pi_{\mu\nu}^{2\mathrm{OPE}}(p)$ for the current $J_{\mu}^{2}(x)$

$$
\begin{aligned}
\Pi_{\mu\nu}^{2\mathrm{OPE}}(p) &= i\int d^4x e^{ipx}\Big\{\mathrm{Tr}\left[\widetilde{S}_c^{b'b}(-x)S_c^{a'a}(-x)\right]\\
&\times\Big[\mathrm{Tr}\left[S_b^{bb'}(x)\gamma_5\gamma_\nu\widetilde{S}_b^{aa'}(x)\gamma_\mu\gamma_5\right]\\
&+\mathrm{Tr}\left[S_b^{ab'}(x)\gamma_5\gamma_\nu\widetilde{S}_b^{ba'}(x)\gamma_\mu\gamma_5\right]\Big]+\mathrm{Tr}\left[S_c^{b'a}(-x)\right.\\
&\left.\times\widetilde{S}_c^{a'b}(-x)\right]\Big[\mathrm{Tr}\left[S_b^{bb'}(x)\gamma_5\gamma_\nu\widetilde{S}_b^{aa'}(x)\gamma_\mu\gamma_5\right]\\
&+\mathrm{Tr}\left[S_b^{ab'}(x)\gamma_5\gamma_\nu\widetilde{S}_b^{ba'}(x)\gamma_\mu\gamma_5\right]\Big]\Big\}. \qquad (13)
\end{aligned}
$$

The spectroscopic parameters m_2 and Λ_2 of this particle are equal to

$$
\begin{aligned}
m_2 &= (13383\pm 92)\ \mathrm{MeV},\\
\Lambda_2 &= (1.01\pm 0.12)\ \mathrm{GeV}^5, \qquad (14)
\end{aligned}
$$

which are obtained by employing the working windows

$$
M^2\in[12,14]\ \mathrm{GeV}^2,\ s_0\in[200,205]\ \mathrm{GeV}^2. \qquad (15)
$$

The pole contribution for $M^2\in[12,14]\ \mathrm{GeV}^2$ on average in s_0 is larger than 0.5 and varies within limits

$$
0.65\geq \mathrm{PC}\geq 0.50. \qquad (16)
$$

At $M^2=12\ \mathrm{GeV}^2$ the nonperturbative contribution is negative and does not exceed 3% of the correlation function. Our predictions for the mass m_2 of the tetraquark T_2 are plotted in Fig. 3.

3. Width of the tetraquark T_1

The mass m_1 of the diquark-antidiquark state T_1 proves that it can decay to $B_c^- B_c^{*-}$ and $B_c^{*-}B_c^{*-}$ mesons. In fact, the mass $m_{B_c}=(6274.47\pm 0.27)$ MeV of the meson B_c^- is known experimentally [42]. For the mass of the vector particle B_c^{*-}, we use the theoretical prediction $m_{B_c^*}=6338$ MeV from Ref. [43]. It is evident, that processes $T_1\to B_c^- B_c^{*-}$ and $T_1\to B_c^{*-}B_c^{*-}$ are kinematically allowed channels for the tetraquark T_1. As the decay constants of B_c^- and B_c^{*-} mesons, we employ $f_{B_c}=(476\pm 27)$ MeV and $f_{B_c^*}=471$ MeV [44,45], respectively.

3.1. Process $T_1\to B_c^- B_c^{*-}$

The width of the decay $T_1\to B_c^- B_c^{*-}$ can be calculated by employing the strong coupling f_1 of particles at the vertex $T_1 B_c^- B_c^{*-}$. To this end, we are going to study the QCD three-point correlation function

$$
\begin{aligned}
\Pi_{\mu\nu}^{1}(p,p') &= i^2\int d^4x d^4y e^{ip'y}e^{-ipx}\langle 0|\mathcal{T}\{J_\mu^{B_c^*}(y)\\
&\times J^{B_c}(0)J_\nu^{1\dagger}(x)\}|0\rangle, \qquad (17)
\end{aligned}
$$

where

$$
\begin{aligned}
J^{B_c}(x) &= \overline{c}_j(x)i\gamma_5 b_j(x),\\
J_\mu^{B_c^*}(x) &= \overline{c}_i(x)\gamma_\mu b_i(x) \qquad (18)
\end{aligned}
$$

are the interpolating currents for the pseudoscalar and vector mesons B_c^- and B_c^{*-}, respectively.

Our aim is to analyze the correlator $\Pi_{\mu\nu}^{1}(p,p')$ and find the sum rule for the form factor $f_1(q^2)$ which at $q^2=m_{B_c}^2$ gives the strong coupling f_1. The SR for $f_1(q^2)$ can be derived by means of usual recipes of the approach. First, we represent $\Pi_{\mu\nu}^{1}(p,p')$ by employing the parameters of T_1 and final-state mesons. The correlation function $\Pi_{\mu\nu}^{1\mathrm{Phys}}(p,p')$ calculated by this way establishes the phenomenological side of SR and has the form

$$
\begin{aligned}
\Pi_{\mu\nu}^{1\mathrm{Phys}}(p,p') &= \frac{\langle 0|J_\mu^{B_c^*}|B_c^*(p',\varepsilon)\rangle}{p'^2-m_{B_c^*}^2}\frac{\langle 0|J^{B_c}|B_c(q)\rangle}{q^2-m_{B_c}^2}\\
&\times\langle B_c^*(p',\varepsilon)B_c(q)|T_1(p,\epsilon)\rangle\frac{\langle T_1(p,\epsilon)|J_\nu^{1\dagger}|0\rangle}{p^2-m_1^2}\\
&+\cdots. \qquad (19)
\end{aligned}
$$

To rewrite $\Pi_{\mu\nu}^{1\mathrm{Phys}}(p,p')$ in a form suitable for further manipulations, we make use of the matrix elements

$$
\begin{aligned}
\langle 0|J^{B_c}|B_c\rangle &= \frac{f_{B_c}m_{B_c}^2}{m_b+m_c},\\
\langle 0|J_\mu^{B_c^*}|B_c^*(p',\varepsilon)\rangle &= f_{B_c^*}m_{B_c^*}\varepsilon_\mu(p'), \qquad (20)
\end{aligned}
$$

where ε_μ is the polarization vector of the meson B_c^{*-}. It is convenient to model the vertex $T_1 B_c^- B_c^{*-}$ in the following form

$$
\begin{aligned}
\langle B_c^*(p',\varepsilon)B_c(q)|T_1(p,\epsilon)\rangle &= f_1(q^2)\left[(p\cdot p')(\epsilon\cdot\varepsilon^*)\right.\\
&\left.-(p'\cdot\epsilon)(p\cdot\varepsilon^*)\right]. \qquad (21)
\end{aligned}
$$

Having determined the required matrix elements, it is not difficult to find that

$$
\begin{aligned}
\Pi_{\mu\nu}^{1\mathrm{Phys}}(p,p') &= f_1(q^2)\frac{\Lambda_1 f_{B_c}m_{B_c}^2 f_{B_c^*}m_{B_c^*}}{(m_b+m_c)\left(p^2-m_1^2\right)\left(p'^2-m_{B_c^*}^2\right)}\\
&\times\frac{1}{(q^2-m_{B_c}^2)}\left(\frac{m_1^2+m_{B_c^*}^2-q^2}{2}g_{\mu\nu}-p_\mu p'_\nu\right)+\cdots. \qquad (22)
\end{aligned}
$$

The correlator $\Pi_{\mu\nu}^{1\mathrm{Phys}}(p,p')$ is a sum of two different Lorentz structures, one of which should be chosen for investigations. We work with the invariant amplitude $\Pi_1^{\mathrm{Phys}}(p^2,p'^2,q^2)$ that corresponds, in Eq. (22), to the structure $g_{\mu\nu}$.

The correlator $\Pi_{\mu\nu}^{1\mathrm{OPE}}(p,p')$, expressed using the quark propagators, reads

$$
\begin{aligned}
\Pi_{\mu\nu}^{1\mathrm{OPE}}(p,p') &= 2i^3\int d^4xd^4y e^{ip'y}e^{-ipx}\left\{\mathrm{Tr}\left[\gamma_5 S_b^{ia}(-x)\right.\right.\\
&\left.\times\gamma_5\sigma_{\nu\theta}\widetilde{S}_b^{jb}(y-x)\gamma_\mu\widetilde{S}_c^{aj}(x-y)\gamma^\theta S_c^{bi}(x)\right]\\
&-\mathrm{Tr}\left[\gamma_5 S_b^{ia}(-x)\gamma_5\sigma_{\nu\theta}\widetilde{S}_b^{jb}(y-x)\gamma_\mu\widetilde{S}_c^{bj}(x-y)\right.
\end{aligned}
$$

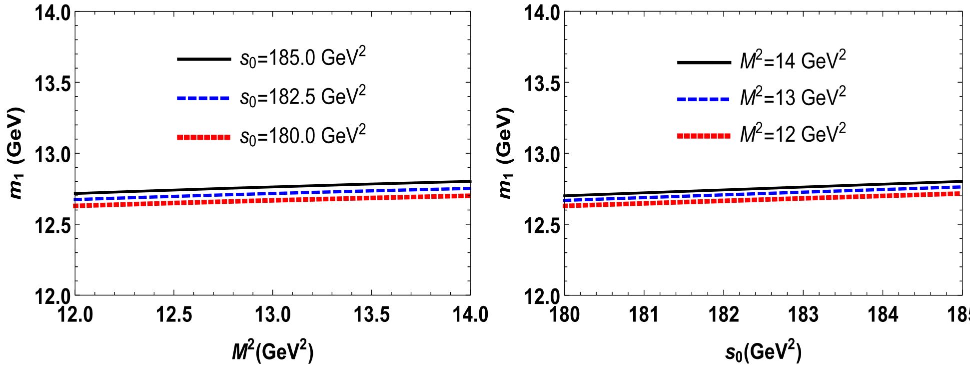

Fig. 2. Mass m_1 of the tetraquark T_1 as a function of the Borel M^2 (left panel), and continuum threshold s_0 parameters (right panel).

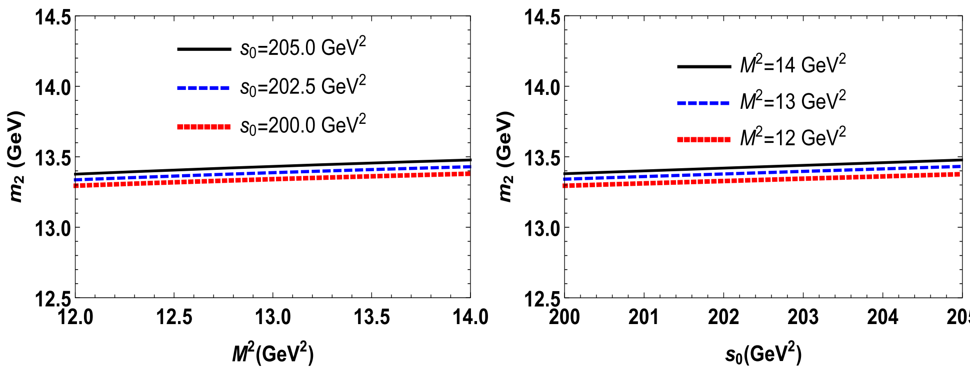

Fig. 3. Dependence of the mass m_2 on the Borel parameter M^2 (left panel), and continuum threshold parameter s_0 (right panel).

$$\times\gamma^{\theta} S_c^{ai}(x)\Big]\Big\}. \tag{23}$$

The $\Pi_{\mu\nu}^{1\mathrm{OPE}}(p,p')$ also consists of two Lorentz structures proportional to $g_{\mu\nu}$ and $p_\mu p'_\nu$, respectively. Having labeled by $\Pi_1^{\mathrm{OPE}}(p^2,p'^2,q^2)$ the amplitude corresponding to the term $g_{\mu\nu}$, we determine the SR for the form factor $f_1(q^2)$

$$f_1(q^2)=\frac{2(m_b+m_c)}{\Lambda_1 f_{B_c} m_{B_c}^2 f_{B_c^*} m_{B_c^*}}\frac{q^2-m_{B_c}^2}{m^2+m_{B_c^*}^2-q^2}$$
$$\times e^{m_1^2/M_1^2} e^{m_{B_c^*}^2/M_2^2}\Pi_1(\mathbf{M}^2,\mathbf{s}_0,q^2). \tag{24}$$

In Eq. (24), $\Pi_1(\mathbf{M}^2,\mathbf{s}_0,q^2)$ is the function $\Pi_1^{\mathrm{OPE}}(p^2,p'^2,q^2)$ after the Borel transformations and continuum subtractions. As a result, it depends on the parameters $\mathbf{M}^2=(M_1^2,M_2^2)$ and $\mathbf{s}_0=(s_0,s'_0)$. The pair (M_1^2,s_0) corresponds to the initial tetraquark channel, whereas (M_2^2,s'_0) describes the B_c^{*-} channel.

In numerical computations for M_1^2 and s_0, we use Eq. (11). The parameters $(M_2^2,\ s'_0)$ for the B_c^{*-} channel are varied inside of the borders

$$M_2^2\in[6.5,7.5]\ \mathrm{GeV}^2,\ s'_0\in[49,51]\ \mathrm{GeV}^2. \tag{25}$$

The sum rule method leads to credible results for the form factor $f_1(q^2)$ in the Euclidean region $q^2<0$. But the strong coupling f_1 is determined by $f_1(q^2)$ at the mass shell $q^2=m_{B_c}^2$. To solve this problem, it is convenient to use the function $f_1(Q^2)$ with $Q^2=-q^2$ and introduce a fit function $\mathcal{F}_1(Q^2,m_1^2)=f_1(Q^2)$ that at momenta $Q^2>0$ coincides with SR data, but can be extended to the domain $Q^2<0$. To this end, we employ the functions

$$\mathcal{F}_i(Q^2,m_1^2)=\mathcal{F}_i^0\exp\left[c_i^1\frac{Q^2}{m_1^2}+c_i^2\left(\frac{Q^2}{m_1^2}\right)^2\right] \tag{26}$$

where $\mathcal{F}_i^0$, c_i^1, and c_i^2 are unknown parameters.

In the present SR computations, Q^2 changes within the interval $Q^2=1-40\ \mathrm{GeV}^2$. The results obtained for $f_1(Q^2)$ are depicted in Fig. 4. Then, by comparing QCD data and Eq. (26), it is not difficult to extract the parameters $\mathcal{F}_1^0=0.38\ \mathrm{GeV}^{-1}$, $c_1^1=2.79$, and $c_1^2=-3.44$ of the function $\mathcal{F}_1(Q^2,m_1^2)$. It is also plotted in Fig. 4, where one sees a nice agreement of $\mathcal{F}_1(Q^2,m_1^2)$ with QCD data.

For the strong coupling f_1, we find

$$f_1\equiv\mathcal{F}_1(-m_{B_c}^2,m_1^2)=(1.6\pm0.2)\times10^{-1}\ \mathrm{GeV}^{-1}. \tag{27}$$

The width of the process $T_1\to B_c^-B_c^{*-}$ is determined by the expression

$$\Gamma\left[T_1\to B_c^-B_c^{*-}\right]=f_1^2\frac{m_{B_c^*}^2\lambda_1}{24\pi}\left(3+\frac{2\lambda_1^2}{m_{B_c^*}^2}\right), \tag{28}$$

where $\lambda_1=\lambda(m_1,m_{B_c^*},m_{B_c})$, and

$$\lambda(x,y,z)=\frac{\sqrt{x^4+y^4+z^4-2(x^2y^2+x^2z^2+y^2z^2)}}{2x}. \tag{29}$$

As a result, we find

$$\Gamma\left[T_1\to B_c^-B_c^{*-}\right]=(32.5\pm8.3)\ \mathrm{MeV}. \tag{30}$$

3.2. Decay $T_1\to B_c^{*-}B_c^{*-}$

To explore the process $T_1\to B_c^{*-}B_c^{*-}$, we start from the correlation function

$$\Pi_{\mu\delta\nu}^1(p,p')=i^2\int d^4x d^4y e^{ip'y}e^{-ipx}\langle0|\mathcal{T}\{J_\mu^{B_c^*}(y)$$
$$\times J_\delta^{B_c^*}(0)J_\nu^{1\dagger}(x)\}|0\rangle. \tag{31}$$

To derive expression of this function in terms of physical parameters of the tetraquark T_1 and B_c^{*-} meson, we write it in the following form

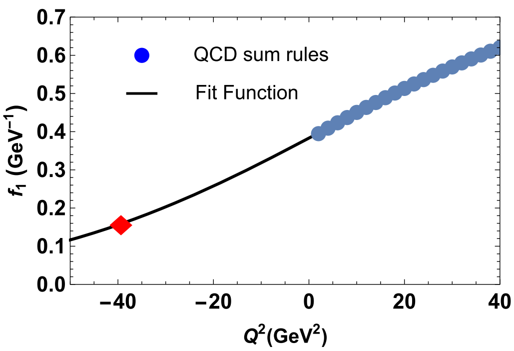

Fig. 4. QCD data and fit function for the form factor $f_1(Q^2)$. The diamond fixes the point $Q^2=-m_{B_c}^2$ where the coupling f_1 has been evaluated.

$$\Pi_{\mu\delta\nu}^{1\mathrm{Phys}}(p,p')=\frac{\langle 0|J_\mu^{B_c^*}|B_c^*(p',\varepsilon(p'))\rangle}{p'^2-m_{B_c^*}^2}\frac{\langle 0|J_\delta^{B_c^*}|B_c^*(q,\varepsilon(q))\rangle}{q^2-m_{B_c^*}^2}$$
$$\times\langle B_c^*(p',\varepsilon(p'))B_c^*(q,\varepsilon(q))|T_1(p,\epsilon)\rangle\frac{\langle T_1(p,\epsilon)|J_\nu^{1\dagger}|0\rangle}{p^2-m_1^2}$$
$$+\cdots. \tag{32}$$

The matrix elements of the B_c^{*-} meson and diquark-antidiquark state T_1 have been defined above. An unknown matrix element here is one connected with the vertex $T_1B_c^{*-}B_c^{*-}$, which we model by means of the expression

$$\langle B_c^*(p',\varepsilon(p'))B_c^*(q,\varepsilon(q))|T_1(p,\epsilon)\rangle=f_2(q^2)\epsilon^{\alpha\beta\gamma\zeta}$$
$$\times\varepsilon_\alpha^*(p')\epsilon_\beta(p)\varepsilon_\gamma^*(q)(p'_\zeta+p_\zeta). \tag{33}$$

The correlator $\Pi_{\mu\gamma\nu}^1(p,p')$ in terms of the physical parameters of the particles T_1 and B_c^{*-} reads

$$\Pi_{\mu\delta\nu}^{1\mathrm{Phys}}(p,p')=\frac{f_2(q^2)\Lambda_1 f_{B_c^*}^2m_{B_c^*}^2}{(p^2-m_1^2)(p'^2-m_{B_c^*}^2)(q^2-m_{B_c^*}^2)}$$
$$\times\left[\epsilon_{\alpha\delta\mu\nu}(p'_\alpha+p_\alpha)+\frac{2p_\alpha p'_\beta\epsilon_{\alpha\beta\mu\nu}(p_\delta-p'_\delta)}{m_{B_c^*}^2}\right.$$
$$\left.+\frac{p_\alpha p'_\beta p'_\mu\epsilon_{\alpha\beta\delta\nu}}{m_{B_c^*}^2}+\frac{p_\alpha p'_\beta p_\nu\epsilon_{\alpha\beta\delta\mu}}{m_1^2}\right]. \tag{34}$$

The same correlation function obtained using the quark propagators has the following form

$$\Pi_{\mu\delta\nu}^{1\mathrm{OPE}}(p,p')=2i^2\int d^4xd^4ye^{ip'y}e^{-ipx}\left\{\mathrm{Tr}\left[\gamma_\delta S_b^{ia}(-x)\right.\right.$$
$$\left.\times\gamma_5\sigma_{\nu\theta}\widetilde{S}_b^{jb}(y-x)\gamma_\mu\widetilde{S}_c^{aj}(x-y)\gamma^\theta S_c^{bi}(x)\right]$$
$$-\mathrm{Tr}\left[\gamma_\delta S_b^{ia}(-x)\gamma_5\sigma_{\nu\theta}\widetilde{S}_b^{jb}(y-x)\gamma_\mu\widetilde{S}_c^{bj}(x-y)\right.$$
$$\left.\left.\times\gamma^\theta S_c^{ai}(x)\right]\right\}. \tag{35}$$

Having used amplitudes corresponding to the structures $\sim\epsilon_{\alpha\delta\mu\nu}p_\alpha$ both in the physical and QCD expressions for the correlation function, one can derive SR for the form factor $f_2(q^2)$.

At the mass shell $q^2=m_{B_c^*}^2$ of the B_c^{*-} meson, the strong coupling f_2 is equal to

$$f_2\equiv\mathcal{F}_2(-m_{B_c^*}^2,m_1^2)=(3.7\pm0.4)\times10^{-1}, \tag{36}$$

which is found by means of the function $\mathcal{F}_2$ with the parameters $\mathcal{F}_2^0=1.1$, $c_2^1=3.53$, and $c_2^2=-3.58$.

The width of the decay $T_1\to B_c^{*-}B_c^{*-}$ is determined by the formula

$$\Gamma\left[T_1\to B_c^{*-}B_c^{*-}\right]=f_2^2\frac{\lambda_2}{48\pi}\left(5+5\xi+\frac{8}{\xi}\right), \tag{37}$$

where $\lambda_2=\lambda(m_1,m_{B_c^*},m_{B_c^*})$ and $\xi=m_1^2/m_{B_c^*}^2$. Then, for the width of this process we get

$$\Gamma\left[T_1\to B_c^{*-}B_c^{*-}\right]=(11.8\pm3.0)\ \mathrm{MeV}. \tag{38}$$

Using information obtained in this section, we get the full width of the tetraquark T_1

$$\Gamma(T_1)=(44.3\pm8.8)\ \mathrm{MeV}, \tag{39}$$

which characterizes it as a relatively narrow resonance.

4. Width of the diquark-antidiquark state T_2

The mass of the axial-vector exotic meson T_2 is large enough and makes possible its decays to the final states $B_c^-B_c^{*-}$, $B_c^{*-}B_c^{*-}$ and $B_c^-(2S)B_c^{*-}$. The meson $B_c^-(2S)$ is a radially excited state of the ground-level particle B_c^-. The mesons B_c^- and $B_c^-(2S)$ are described by the same interpolating current J^{B_c}. This means that the physical side of the sum rule for the strong coupling F_2 at the vertex $T_2B_c^-(2S)B_c^{*-}$ necessarily contains a term corresponding to the vertex $T_2B_c^-B_c^{*-}$ with coupling F_1. Contributions of these two terms can be separated by choosing an appropriate s_0, i.e., by fixing $s_0<\widetilde{m}_{B_c}^2$ with $\widetilde{m}_{B_c}$ being the mass of the meson $B_c^-(2S)$, we can include effects of F_2 into "higher resonances and continuum states". Then, it is not difficult to determine the coupling F_1, and use it as an input parameter in the sum rule with $s_0>\widetilde{m}_{B_c}^2$ to extract F_2. Below, we follow namely this strategy.

4.1. $T_2\to B_c^-B_c^{*-}$ and $T_2\to B_c^-(2S)B_c^{*-}$

The correlation function necessary to obtain the form factors $F_1(q^2)$ and $F_2(q^2)$ at the vertices $T_2B_c^-B_c^{*-}$ and $T_2B_c^-(2S)B_c^{*-}$ is given by the formula

$$\Pi_{\mu\nu}^2(p,p')=i^2\int d^4xd^4ye^{ip'y}e^{-ipx}\langle 0|\mathcal{T}\{J^{B_c}(y)$$
$$\times J_\mu^{B_c^*}(0)J_\nu^\dagger(x)\}|0\rangle. \tag{40}$$

The physical side of SRs for $F_1(q^2)$ and $F_2(q^2)$ is determined by the expression

$$\Pi_{\mu\nu}^{2\mathrm{Phys}}(p,p')=\frac{\Lambda_2 f_{B_c^*}m_{B_c^*}}{(m_b+m_c)\left(p^2-m_2^2\right)\left(q^2-m_{B_c^*}^2\right)}$$
$$\times\left[F_1(q^2)\frac{f_{B_c}m_{B_c}^2}{(p'^2-m_{B_c}^2)}\left(\frac{m_2^2-m_{B_c}^2+q^2}{2}g_{\mu\nu}-p_\mu q_\nu\right)\right.$$
$$\left.+F_2(q^2)\frac{\widetilde{f}_{B_c}\widetilde{m}_{B_c}^2}{(p'^2-\widetilde{m}_{B_c}^2)}\left(\frac{m_2^2-\widetilde{m}_{B_c}^2+q^2}{2}g_{\mu\nu}-p_\mu q_\nu\right)\right]$$
$$+\cdots. \tag{41}$$

Here, $\widetilde{m}_{B_c}=(6871.2\pm1.0)$ MeV and $\widetilde{f}_{B_c}=(420\pm20)$ MeV are parameters of the meson $B_c^-(2S)$ borrowed from Refs. [42,46], respectively.

The QCD side of the SRs is:

$$\Pi_{\mu\nu}^{2\mathrm{OPE}}(p,p')=2i\int d^4xd^4ye^{ip'y}e^{-ipx}\left\{\mathrm{Tr}\left[\gamma_\mu S_b^{ja}(-x)\right.\right.$$
$$\left.\times\gamma_5\gamma_\nu\widetilde{S}_b^{ib}(y-x)\gamma_5\widetilde{S}_c^{ai}(x-y)S_c^{bj}(x)\right]$$
$$\left.-\mathrm{Tr}\left[\gamma_\mu S_b^{ja}(-x)\gamma_5\gamma_\nu\widetilde{S}_b^{ib}(y-x)\gamma_5\widetilde{S}_c^{bi}(x-y)S_c^{aj}(x)\right]\right\}. \tag{42}$$

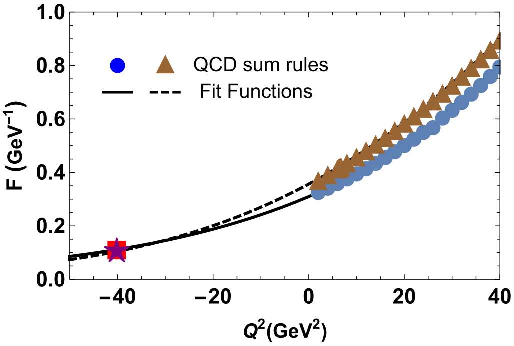

Fig. 5. QCD data and extrapolating functions $\mathcal{G}_1(Q^2)$ (solid line) and $\mathcal{G}_2(Q^2)$ (dashed line). The star and square show the points $Q^2=-m^2_{B_c^*}$ where the couplings F_1 and F_2 have been computed.

The functions $\Pi^{\rm 2Phys}_{\mu\nu}(p,p')$ and $\Pi^{\rm 2OPE}_{\mu\nu}(p,p')$ have two Lorentz structures proportional to $g_{\mu\nu}$ and $p_\mu q_\nu$. In what follows, we employ the amplitudes $\sim g_{\mu\nu}$ to find SR for the form factors $F_1(q^2)$ and $F_2(q^2)$. We equate, as usual, the invariant amplitudes $\Pi_2^{\rm Phys}(p^2,p'^2,q^2)$ and $\Pi_2^{\rm OPE}(p^2,p'^2,q^2)$ corresponding to these structures and find an expression which contains two unknown functions $F_1(q^2)$ and $F_2(q^2)$.

We divide determination of the form factors $F_1(q^2)$ and $F_2(q^2)$ by means of a SR equality into two stages. As the first step, we consider $F_1(q^2)$, and employ a result obtained for this form factor at the second stage to calculate $F_2(q^2)$. In both stages of analysis, we use for (M_1^2,s_0) the parameters of Eq. (15). These two phases are distinguished by the regions chosen for the parameters (M_2^2,s_0'). At first, we limit s_0' by the mass of the meson $B_c^-(2S)$ and fix $s_0'<\widetilde{m}^2_{B_c}$. This allows us to treat the contribution of the vertex $T_2B_c^-B_c^{*-}(2S)$ as "a continuum effect" and explore only the first component in Eq. (41). The parameters (M_2^2,s_0') are determined by the expression

$$M_2^2\in[6.5,7.5]~\mathrm{GeV}^2,~s_0'\in[45,47]~\mathrm{GeV}^2. \tag{43}$$

The form factor $F_1(q^2)$ can be modeled by the fit function $\mathcal{G}_1(Q^2,m_2^2)$ with parameters $\mathcal{G}_1^0=0.31~\mathrm{GeV}^{-1}$, $g_1^1=4.39$ and $g_1^2=-0.74$ (see, Fig. 5). Let us note that the functions $\mathcal{G}_j(Q^2,m_2^2)$ have the analytic form of Eq. (26) with substitutions $m_1^2\to m_2^2$ and $\mathcal{F}_j^0$, $c_j^{1(2)}\to\mathcal{G}_j^0$, $g_j^{1(2)}$, respectively.

The strong coupling F_1 computed at the mass shell $q^2=m^2_{B_c^*}$ of the B_c^{*-} meson is equal to

$$F_1\equiv\mathcal{G}_1(-m^2_{B_c^*},m_2^2)=(1.1\pm0.1)\times10^{-1}~\mathrm{GeV}^{-1}. \tag{44}$$

At the next step, we choose

$$M_2^2\in[6.5,7.5]~\mathrm{GeV}^2,~s_0^{*\prime}\in[48,50]~\mathrm{GeV}^2, \tag{45}$$

and utilize $F_1(q^2)$ as an input to extract the form factor $F_2(q^2)$, where $s_0^{*\prime}$ is limited by the mass of the meson $B_c(3S)$, i.e., $m^2[B_c(3S)]=(7.272)^2~\mathrm{GeV}^2$ [43]. Analysis carried out in the context of this approach leads to the result

$$F_2\equiv\mathcal{G}_2(-m^2_{B_c^*},m_2^2)=(1.0\pm0.1)\times10^{-1}~\mathrm{GeV}^{-1}, \tag{46}$$

where $\mathcal{G}_2(-m^2_{B_c^*},m_2^2)$ is determined by the parameters $\mathcal{G}_2^0=0.36~\mathrm{GeV}^{-1}$, $g_2^1=4.81$ and $g_2^2=-3.01$. Relevant information is shown graphically in Fig. 5.

The width of the decays $T_2\to B_c^-B_c^{*-}$ and $T_2\to B_c^-(2S)B_c^{*-}$, after necessary refinements, can be computed using Eq. (28):

$$\Gamma\left[T_2\to B_c^-B_c^{*-}\right]=(48.1\pm12.2)~\mathrm{MeV},$$
$$\Gamma\left[T_2\to B_c^-(2S)B_c^{*-}\right]=(19.0\pm4.8)~\mathrm{MeV}. \tag{47}$$

4.2. $T_2\to B_c^{*-}B_c^{*-}$

This process is investigated as the decay $T_1\to B_c^{*-}B_c^{*-}$ considered in the previous section, differences being in the mass m_2, correlation function $\Pi^{\rm 2OPE}_{\mu\delta\nu}(p,p')$ and strong coupling F_3 at the vertex $T_2B_c^{*-}B_c^{*-}$.

The physical side of SR for the form factor $F_3(q^2)$, after some replacements, is determined by the expression Eq. (34). But the function $\Pi^{\rm 2OPE}_{\mu\delta\nu}(p,p')$ due to the current $J^2_\mu(x)$ takes the following form

$$\Pi^{\rm 2OPE}_{\mu\delta\nu}(p,p')=2i^2\int d^4xd^4ye^{ip'y}e^{-ipx}\Big\{\mathrm{Tr}\left[\gamma_\delta S_b^{ia}(-x)\right.$$
$$\left.\times\gamma_5\gamma_\nu\widetilde{S}_b^{jb}(y-x)\gamma_\mu\widetilde{S}_c^{aj}(x-y)S_c^{bi}(x)\right]$$
$$+\mathrm{Tr}\left[\gamma_\delta S_b^{ia}(-x)\gamma_5\gamma_\nu\widetilde{S}_b^{jb}(y-x)\gamma_\mu\widetilde{S}_c^{bj}(x-y)S_c^{ai}(x)\right]\Big\}. \tag{48}$$

Remaining manipulations are standard ones, therefore below we provide the final results obtained for this mode. The coupling F_3 is computed at the mass shell of the B_c^{*-} meson by means of the extrapolating function $\mathcal{G}_3(-m^2_{B_c^*},m_2^2)$ with parameters $\mathcal{G}_3^0=11.79$, $g_3^1=13.67$ and $g_3^2=-20.84$. It is equal to

$$F_3\equiv\mathcal{G}_3(-m^2_{B_c^*},m_2^2)=(1.9\pm0.2)\times10^{-1}. \tag{49}$$

The partial width of the decay $T_2\to B_c^{*-}B_c^{*-}$ is

$$\Gamma\left[T_2\to B_c^{*-}B_c^{*-}\right]=(15.4\pm3.9)~\mathrm{MeV}. \tag{50}$$

Then, one can easily estimate the full width of the tetraquark T_2

$$\Gamma(T_2)=(82.5\pm13.7)~\mathrm{MeV}. \tag{51}$$

5. Concluding notes

We have investigated the axial-vector tetraquarks $bb\overline{c}\overline{c}$ by modeling them as diquark-antidiquark states composed of a diquark $b^TC\sigma_{\mu\nu}\gamma_5b$ and antidiquark $\overline{c}\gamma^\nu C\overline{c}^T$ (T_1) and a vector diquark and pseudoscalar antidiquark (T_2), respectively. The structures T_1 and T_2 have color triplet $\overline{\mathbf{3}}_c\otimes\mathbf{3}_c$ and sextet $\mathbf{6}_c\otimes\overline{\mathbf{6}}_c$ organizations, respectively. Our predictions $m_1=(12714\pm86)$ MeV and $m_2=(13383\pm92)$ MeV prove that these tetraquarks are unstable against the strong decays. In this aspect, our conclusions are in accord with ones made in Refs. [31,33–35]. But, we could not confirm predictions made in Refs. [36,37] about the strong-interaction stable nature some of the axial-vector particles $bb\overline{c}\overline{c}$.

The results for the masses of the structures T_1 and T_2 have permitted us to reveal their possible decay modes. The full width of the exotic mesons T_1 and T_2 are evaluated by computing partial widths of the decays $T_1\to B_c^-B_c^{*-}$, $B_c^{*-}B_c^{*-}$ and $T_2\to B_c^-B_c^{*-}$, $B_c^{*-}B_c^{*-}$ and $T_2\to B_c^-(2S)B_c^{*-}$, respectively. Predictions for the full widths of the axial-vector tetraquarks $\Gamma(T_1)=(44.3\pm8.8)$ MeV and $\Gamma(T_2)=(82.5\pm13.7)$ MeV mean that they may be interpreted as states with modest widths.

As is seen there are controversial results for the parameters of the $bb\overline{c}\overline{c}/cc\overline{b}\overline{b}$ tetraquarks with spin-parities $J^{\rm P}=0^+$, 1^+ and 2^+. Additionally, our analyses do not encompass all possible axial-vector states which may be composed using diquarks (antidiquarks) with different quantum numbers. Such structures may be also studied in the sum rule framework. Because the four-quark compounds $bb\overline{c}\overline{c}/cc\overline{b}\overline{b}$ did not yet discovered experimentally, it is difficult to make conclusions about features of such particles. They may be pure T_1 or T_2 states and bear parameters of these structures. Alternatively, physical resonances may be a superposition of these and other basic states.

In any case, further experimental and theoretical studies of multiquark mesons $bb\overline{c}\overline{c}/cc\overline{b}\overline{b}$ are required for reliable statements concerning parameters of such tetraquarks. Our present analysis is a useful step in this direction.

Declaration of competing interest

We declare that there is no conflict of interests regarding this manuscript.

Data availability

No data was used for the research described in the article.

Acknowledgements

K. Azizi is thankful to Iran National Science Foundation (INSF) for the partial financial support provided under the elites Grant No. 4025036.

References

[1] R. Aaij, et al., LHCb Collaboration, Sci. Bull. 65 (2020) 1983.
[2] E. Bouhova-Thacker, ATLAS Collaboration, in: PoS ICHEP2022, 2022, p. 806.
[3] A. Hayrapetyan, et al., CMS Collaboration, arXiv:2306.07164 [hep-ex].
[4] J.R. Zhang, Phys. Rev. D 103 (2021) 014018.
[5] R.M. Albuquerque, S. Narison, A. Rabemananjara, D. Rabetiarivony, G. Randriamanatrika, Phys. Rev. D 102 (2020) 094001.
[6] B.C. Yang, L. Tang, C.F. Qiao, Eur. Phys. J. C 81 (2021) 324.
[7] C. Becchi, A. Giachino, L. Maiani, E. Santopinto, Phys. Lett. B 806 (2020) 135495.
[8] C. Becchi, A. Giachino, L. Maiani, E. Santopinto, Phys. Lett. B 811 (2020) 135952.
[9] Z.G. Wang, Nucl. Phys. B 985 (2022) 115983.
[10] R.N. Faustov, V.O. Galkin, E.M. Savchenko, Symmetry 14 (2022) 2504.
[11] P. Niu, Z. Zhang, Q. Wang, M.L. Du, Sci. Bull. 68 (2023) 800.
[12] W.C. Dong, Z.G. Wang, Phys. Rev. D 107 (2023) 074010.
[13] G.L. Yu, Z.Y. Li, Z.G. Wang, J. Lu, M. Yan, Eur. Phys. J. C 83 (2023) 416.
[14] S.Q. Kuang, Q. Zhou, D. Guo, Q.H. Yang, L.Y. Dai, Eur. Phys. J. C 83 (2023) 383.
[15] S.S. Agaev, K. Azizi, B. Barsbay, H. Sundu, Phys. Lett. B 844 (2023) 138089.
[16] S.S. Agaev, K. Azizi, B. Barsbay, H. Sundu, Eur. Phys. J. Plus 138 (2023) 935.
[17] S.S. Agaev, K. Azizi, B. Barsbay, H. Sundu, Nucl. Phys. A 844 (2024) 122768.
[18] S.S. Agaev, K. Azizi, B. Barsbay, H. Sundu, Eur. Phys. J. C 83 (2023) 994.
[19] S.S. Agaev, K. Azizi, B. Barsbay, H. Sundu, Phys. Rev. D 109 (2024) 014006.
[20] Z.G. Wang, X.S. Yang, AAPPS Bull. 34 (2024) 5.
[21] X.K. Dong, V. Baru, F.K. Guo, C. Hanhart, A. Nefediev, Phys. Rev. Lett. 126 (2021) 132001, Phys. Rev. Lett. 127 (2021) 119901(E).
[22] Z.R. Liang, X.Y. Wu, D.L. Yao, Phys. Rev. D 104 (2021) 034034.
[23] W. Chen, H.X. Chen, X. Liu, T.G. Steele, S.L. Zhu, Phys. Rev. D 95 (2017) 114005.
[24] S.S. Agaev, K. Azizi, H. Sundu, Eur. Phys. J. C 78 (2018) 141.
[25] S.S. Agaev, K. Azizi, B. Barsbay, H. Sundu, Nucl. Phys. B 939 (2019) 130.
[26] S.S. Agaev, K. Azizi, H. Sundu, Phys. Lett. B 820 (2021) 136530.
[27] R. Aaij, et al., LHCb Collaboration, Phys. Rev. Lett. 131 (2023) 041902.
[28] R. Aaij, et al., LHCb Collaboration, Phys. Rev. D 108 (2023) 012017.
[29] S.S. Agaev, K. Azizi, H. Sundu, Phys. Rev. D 93 (2016) 094006.
[30] W. Chen, H.X. Chen, X. Liu, T.G. Steele, S.L. Zhu, Phys. Rev. Lett. 117 (2016) 022002.
[31] J. Wu, Y.R. Liu, K. Chen, X. Liu, S.L. Zhu, Phys. Rev. D 97 (2018) 094015.
[32] G. Li, X.F. Wang, Y. Xing, Eur. Phys. J. C 79 (2019) 645.
[33] G.J. Wang, L. Meng, S.L. Zhu, Phys. Rev. D 100 (2019) 096013.
[34] M.S. Liu, Q.F. Lü, X.H. Zhang, Q. Zhao, Phys. Rev. D 100 (2019) 016006.
[35] V.O. Galkin, E.M. Savchenko, arXiv:2310.20247 [hep-ph].
[36] Q.N. Wang, Z.Y. Yang, W. Chen, H.X. Chen, Phys. Rev. D 104 (2021) 014040.
[37] H. Mutuk, Phys. Lett. B 834 (2022) 137404.
[38] S.S. Agaev, K. Azizi, B. Barsbay, H. Sundu, arXiv:2311.10534 [hep-ph].
[39] M.A. Shifman, A.I. Vainshtein, V.I. Zakharov, Nucl. Phys. B 147 (1979) 385.
[40] M.A. Shifman, A.I. Vainshtein, V.I. Zakharov, Nucl. Phys. B 147 (1979) 448.
[41] S.S. Agaev, K. Azizi, H. Sundu, Turk. J. Phys. 44 (2020) 95.
[42] R.L. Workman, et al., Particle Data Group, Prog. Theor. Exp. Phys. 2022 (2022) 083C01.
[43] S. Godfrey, Phys. Rev. D 70 (2004) 054017.
[44] E.V. Veliev, K. Azizi, H. Sundu, N. Aksit, J. Phys. G 39 (2012) 015002.
[45] E.J. Eichten, C. Quigg, Phys. Rev. D 99 (2019) 054025.
[46] T.M. Aliev, T. Barakat, S. Bilmis, Nucl. Phys. B 947 (2019) 114726.